Available online at www.sciencedirect.com
SCIENCE DIRECT®
Biology of the Cell 94 (2002) 501–510
Biology of the Cell
www.elsevier.com/locate/bicell

Review

The electrophysiology of gap junctions and gap junction channels and their mathematical modelling

Rolf Vogel [a], Robert Weingart [b,*]

[a] *Department of Cardiology, Swiss Cardiovascular Center Inselspital CH-3010 Bern, Switzerland*
[b] *Department of Physiology University of Bern Bühlplatz 5 CH-3012 Bern, Switzerland*

Received 22 March 2002; accepted 15 October 2002

Abstract

In most tissues of vertebrates, gap junctions control the exchange of ions and small molecules between adjacent cells, thus co-ordinating the cellular activities. The application of the dual voltage-clamp method to cell pair preparations enables one to elucidate the electrical properties of gap junctions and gap junction channels. The conductive and kinetic data obtained at the multichannel and single channel level led to a generalised concept for the operation of gap junction channels. Based on the biological data gained in this way, a mathematical model has been developed. This model is versatile and allows to simulate the electrophysiological behaviour of different types of vertebrate gap junctions.

Keywords: Gap junction; Connexins; Electrophysiology; Mathematical model; Simulation

1. Introduction

Gap junctions are pathways through which ions and small molecules are exchanged between adjacent cells. Hence, they provide a means to co-ordinate the cellular activity in tissues. This option has been utilised by metazoa of divergent phylogenetic species and at different ontogenetic stages. As a result, gap junctions are critically involved in a wide spectrum of biological processes including development, growth, secretion and impulse propagation. From a structural point of view, gap junctions are assemblies of intercellular channels (gap junction channels). Each channel consists of two hemichannels (connexons) and each connexon accommodates six transmembrane proteins (connexins), which form an aqueous pore. Over the last decade, molecular biologists have identified 17 different vertebrate connexins encoded by a multigene family (Kumar, 1999; see also Condorelli et al., 1998; Sohl et al., 1998). Hydropathy plots predict a topology with four transmembrane regions (M1–M4), two extracellular loops (E1, E2) and three cytoplasmic portions, i.e. the amino-terminal (NT), a cytoplasmic loop (CL) and the carboxy-terminal (CT). The molecular mass of connexins ranges from 26 to 60 kDa. This variation is accounted for by different lengths of the CL and CT segment of the molecule. Sequence analyses indicated a significant amount of overall similarity (35–65%), the variability mainly being caused by the CT segment. Three-dimensional (3D) density maps from crystals of recombinant channel proteins provided further insight into the structural organisation of gap junction channels (Unger et al., 1999). Apposing connexons are staggered by about 30° while M1–M4 form transmembrane rods of α-helical conformation, one lining the pore and one in close contact with the membrane lipids. Functional analysis associated with mutagenesis provided first hints towards a general structure–function relationship of Cx channels. M3 has an amphipathic character and hence may be the pore-lining segment, NT most likely contains the sensor for V_j-gating (Purnick et al., 2000), CT plays a key role in pH-gating (Ek-Vitorin et al., 1996), and E1 seems to be involved in channel selectivity (Trexler et al., 2000).

This chapter elaborates on representative electrophysiological data which provide the basis for the current concept of the operation of gap junction channels (for a comprehensive review on the biophysics of gap junction channels, see Harris, 2001). To elucidate the subtle properties of the channels, our generalised mathematical model will be brought up (Vogel and Weingart, 1998). The terms multichannel and

* Corresponding author. Tel.: +41-31-631-8706; fax: +41-31-631-4611.
E-mail address: weingart@pyl.unibe.ch (R. Weingart)

PII: S0248-4900(02)00022-9

single channel will be used synonymously for gap junctions and gap junction channels, respectively. To allude to connexins, we will use the nomenclature by species of origin and molecular mass.

2. Biological measurements

2.1. Multichannel currents

In many tissues, the cells express more than one type of connexin (Bruzzone et al., 1996). This opens the possibility of forming a variety of structurally different channels. Hemichannels may contain one type of connexin (homomeric) or more than one type (heteromeric) while gap junction channels may consist of two identical hemichannels (homotypic) or two different hemichannels (heterotypic). Hence, gap junction channels can be homomeric-homotypic, heteromeric-homotypic, homomeric-heterotypic or heteromeric-heterotypic. This spectrum of channels renders it difficult to study the properties of identified types of channels.

To deal with this situation, electrophysiologists have used expression systems such as mRNA-injected oocytes or cDNA-transfected cells of communication deficient cell lines to perform cell pair experiments with the dual voltage-clamp method (Waltzmann et al., 1995; Bruzzone et al., 1996). Fig. 1 illustrates the general behaviour of a homomeric-homotypic gap junction (Fig. 1A,C; cells 1 and 2 express Cx40) and a homomeric-heterotypic gap junction (Fig. 1B,D; cell 1 expresses Cx32, cell 2 expresses Cx26). Application of a transjunctional voltage, V_j ($V_j = V_2 - V_1$), produces a junctional current, I_j. In the homomeric-homotypic case, I_j is symmetrical with regard to V_j polarity and inactivates partially with time (Fig. 1A). In the homomeric-heterotypic case, I_j is asymmetrical, i.e. it inactivates partially with time in the presence of only one V_j polarity (Fig. 1B). To obtain a complete description of the voltage sensitivity of g_j, V_j has to be altered in a systematic manner. For analysis, the amplitude of I_j is determined at the beginning ($I_{j,inst}$; inst, instantaneous) and end ($I_{j,ss}$; ss, steady state) of each V_j pulse to calculate the conductances $g_{j,inst} = I_{j,inst}/V_j$ and $g_{j,ss} = I_{j,ss}/V_j$, respectively. The normalised values of $g_{j,inst}$ (open circles) and $g_{j,ss}$ (filled circles) are then plotted

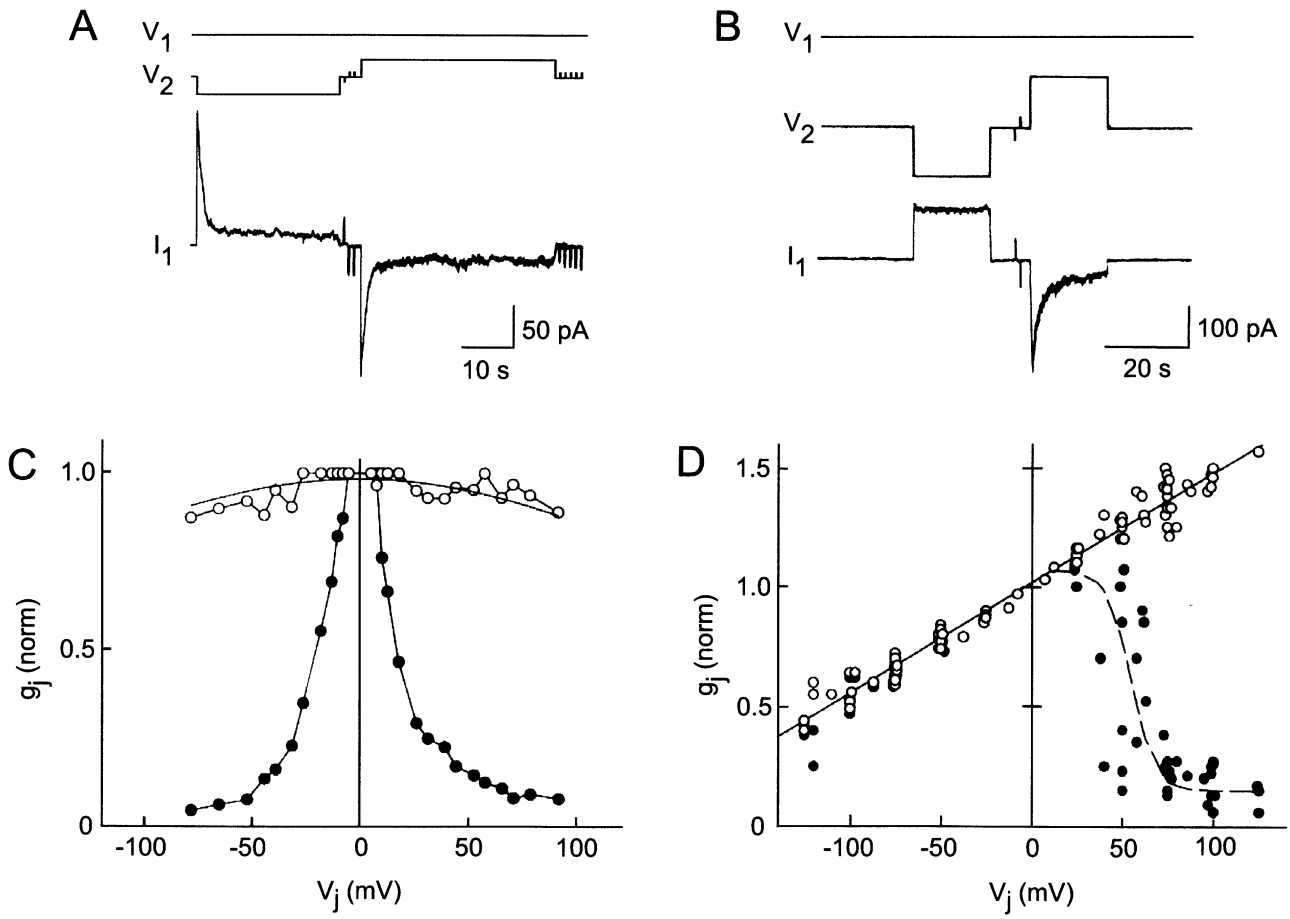

Fig. 1. Dependence of gap junction conductance, g_j, on transjunctional voltage, V_j, determined in a pair of HeLa cells. (A) cells 1 and 2 express Cx40; (B) cell 1 expresses Cx32, cell 2 expresses Cx26. (A, B) V_1 and V_2: pulse protocol giving rise to a V_j of –100 mV (left-hand side) and 100 mV (right-hand side); I_2: junctional current exhibiting a time-dependent decay. (C, D) normalised relationships $g_{j,inst} = f(V_j)$ (open circles) and $g_{j,ss} = f(V_j)$ (filled circles) [panels A and C from Bukauskas et al., 1995a; panels B and D from Bukauskas et al., 1995b].

vs. V_j. In the case of homotypic gap junctions, $g_{j,inst} = f(V_j)$ and $g_{j,ss} = f(V_j)$ are symmetrical with respect to the polarity of V_j (Fig. 1C). The former function is virtually constant. The latter is bell-shaped and best described by the Boltzmann function applied separately for each voltage polarity, assuming that each channel contains two symmetrical gates in series (Harris et al., 1981). At $V_j = 0$ mV, $g_{j,ss}$ is maximal. It decreases as V_j increases, however, without reaching zero. For heterotypic gap junctions, $g_{j,inst} = f(V_j)$ and $g_{j,ss} = f(V_j)$ are both asymmetrical (Fig. 1D). The former shows a nearly linear dependence on V_j, i.e. $g_{j,inst}$ increases with positive V_j and decreases with negative V_j. The latter exhibits a more complex behaviour. At positive V_j, $g_{j,ss}$ declines in a sigmoidal fashion to a level different from zero. At negative V_j, $g_{j,ss}$ fails to show a sigmoidal decay. Instead, it follows the $g_{j,inst}$ relationship. Based on such electrophysiological studies, gap junctions can be characterised by sets of Boltzmann parameters, i.e. the voltage at which $g_{j,ss}$ is half-maximally inactivated, $V_{j,0}$, the normalised conductance at large V_j, $g_{j,min}$, and the number of unitary positive charges moving through the electric field applied, z (Harris et al., 1981). For example, in the case of homomeric-homotypic channels, $V_{j,0}$ varies from ±16 mV (Cx37) to ±90 mV (Cx26) while $g_{j,min}$ is about 0.2 (Waltzmann et al., 1995).

2.2. Single channel currents

To gain further insight into the electrophysiological properties of gap junctions, investigators have resorted to the measurement of current flow through single gap junction channels. Since studies on pairs of oocytes do not allow to resolve unitary currents, transfected cells had to be used. However, a problem with these cells is that their gap junctions usually consist of many channels. Hence, analyses of single channel events cannot be accomplished readily. To render such cell pairs suitable for single channel experiments, the number of operational channels must be reduced. A widely used method involves exposure to submaximal doses of lipophilic agents such as long-chain *n*-alkanols (Rüdisüli and Weingart, 1989; Valiunas et al., 1997). Yet, these interventions introduce new problems because they themselves affect the properties under investigation.

To circumvent these difficulties, we have used an induced cell pair approach. This technique involves pushing two single cells against each other to establish a physical cell-to-cell contact, and the subsequent de novo formation of gap junction channels. Initially, this method has been used to investigate gap junctions of an insect cell line (Bukauskas and Weingart, 1994). This choice turned out to be fortunate because channels formed quickly (~5 min) and had large unitary conductance (375 pS). Once experienced with this method, we have applied this method to transfected human HeLa cells (Bukauskas et al., 1995a) and dispersed neonatal rat heart cells (Valiunas et al., 1997).

Fig. 2A illustrates the genesis of a gap junction channel between two HeLa cells expressing Cx40 during the application of a maintained V_j. The first current transition is slow (~40 ms) and reflects the first opening of a newly formed channel. The slow transitions occasionally show discrete current levels suggesting the sequential operation of subgates. The current then settles at a stable level equivalent to the main open state of the channel. The subsequent transitions are fast (<2 ms, i.e. within the frequency response of the set-up) and result from V_j-dependent gating. During this mode of activity, I_j does not return to the reference level. Instead, it flickers between two levels corresponding to the main state and residual state (dashed line). The latter reflects incomplete channel closure, a phenomenon first described by

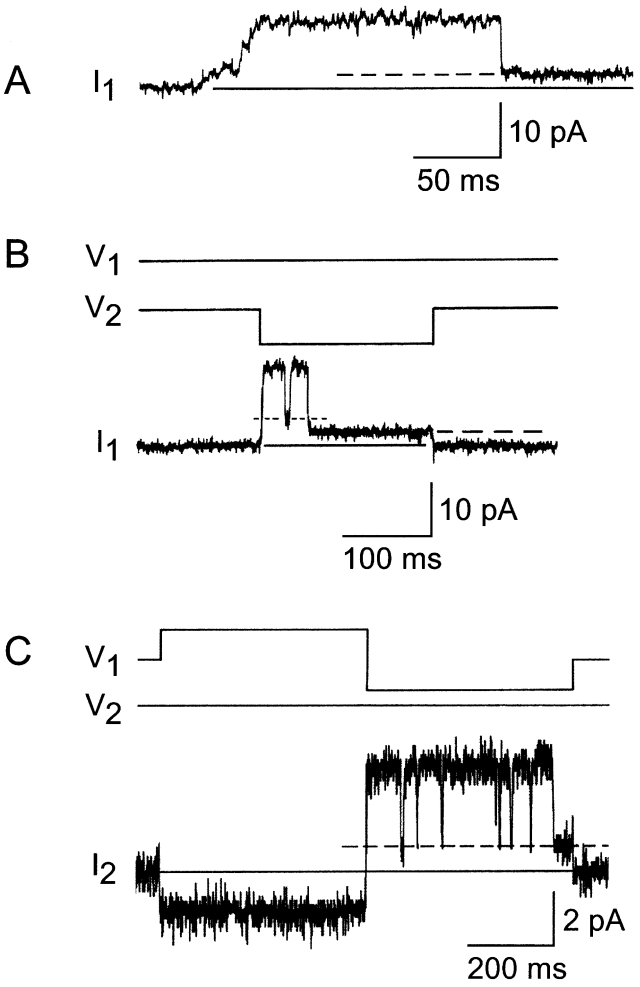

Fig. 2. Single channel currents recorded from induced pairs of transfected HeLa cells. (A) de novo formation of a gap junction channel between two cells expressing Cx40. I_1: junctional current associated with a maintained V_j of –65 mV (V_1 = –50 mV; V_2 = –115 mV; signals not shown). Solid line: zero current reference level; dashed line: residual current level. The first sign of channel insertion was apparent 35 min after establishing a cell-to-cell contact. (B) homomeric-homotypic gap junction channel (Cx40) exhibiting a main state, substates (I_1, pointed lines) and a residual state (I_1, dashed lines). V_j pulse of –75 mV (V_1 = –50 mV; V_2 = –125 mV). (C) homomeric-heterotypic gap junction channel (cell 1: Cx32, cell 2: Cx26) exhibiting a V_j-sensitive $\gamma_{j,main}$. Bipolar V_j pulse of ±50 mV (V_1 = 0 mV/–100 mV, V_2 = –50 mV); $\gamma_{j,main}$ = 80/30 pS, $\gamma_{j,residual}$ = 19 pS/not present (for positive/negative V_j) [panels A and B from Bukauskas et al., 1995a; panel C from Bukauskas et al., 1995b].

Bukauskas and Weingart (1994). Insertion of additional channels follows the same pattern (not shown). Hence, the sequence '*slow channel opening, followed by fast flickering*' provides an engram to identify newly formed channels. Recruitment of channels leads to a sigmoidal increase of g_j with time, indicating that channel insertion is a co-operative process. Gap junction formation usually is complete within 10–30 min.

The time window between the first and second channel insertion is suitable for further exploring the properties of single channels (Fig. 2B; HeLa cells expressing Cx40). Repetitive application of voltage pulses (V_2) occasionally reveals I_j signals with additional discrete levels interposed between $I_{j,main}$ and $I_{j,residual}$ (dashed line). Hence, they are attributable to substates (pointed line). Transitions between the main state, the substates and the residual state are typically fast (<2 ms). Substates are preferentially seen early during large V_j pulses. Their lifetime is short, i.e. usually less than 30 ms (Bukauskas et al., 1995a). Substates are consistent with the presence of subgates.

The values of $\gamma_{j,main}$ for homomeric-homotypic channels obtained in this way range from 45 pS for Cx32 to 460 pS for Cx37 (Bukauskas et al., 1995b; Bukauskas and Weingart, unpublished). The values of $\gamma_{j,residual}$ are 10 and 100 pS, respectively. Hence, the ratio $\gamma_{j,main}/\gamma_{j,residual}$ is 4.5 and 4.6, respectively. To examine unitary currents, many authors have used cell pairs treated with uncoupling agents (Waltzman and Spray, 1995). Because this approach does not allow to distinguish between $I_{j,main}$ and $(I_{j,main} - I_{j,residual})$, data comparison should be done with caution (Bukauskas and Weingart, 1994).

Newly formed cell pairs with a single operational gap junction channel are also useful to examine the channel kinetics at steady state. Such studies indicate that the probability of a channel to be in the main state, P_o, decreases with increasing V_j. The function $P_o = f(V_j)$ decreases from 1 to 0 in a sigmoidal manner (Bukauskas et al., 1995a; Valiunas et al., 1999a). Hence, g_j at large V_j (see Fig. 1A) cannot be explained by a partial decrease in P_o. Conceivably, it reflects the presence of $\gamma_{j,residual}$.

We have also employed induced cell pairs to study the properties of single homomeric-heterotypic channels. Fig. 2C illustrates such an example (cell 1: Cx32; cell 2: Cx26) using a bipolar pulse protocol. It shows that the single channel current is dependent on the polarity of V_j. The amplitude of I_j is smaller for negative V_j (left-hand side) than for positive V_j (right-hand side) indicating that the channel is rectifying. Moreover, the latter exhibits a residual current (dashed line), but not the former one. The application of V_j pulses of different amplitudes and of either polarity reveals that $\gamma_{j,main} = f(V_j)$ can be approximated by a straight line with positive slope (Bukauskas et al., 1995b). Since $\gamma_{j,main}$ of Cx26-Cx26 channels is larger than $\gamma_{j,main}$ of Cx32–Cx32 channels (140 vs. 45 pS), it follows from Kirchhoff's law that $\gamma_{j,main}$ of a Cx26–Cx32 channel is predominantly determined by the properties of the Cx32 hemichannel. Hence, the rectification of the Cx26–Cx32 channel may be brought about by a voltage-dependent conductance of the Cx32 hemichannel. The prediction that hemichannels exhibit such a property has been confirmed later on by direct measurements on gap junction hemichannels (Trexler et al., 1996; Valiunas and Weingart, 2000; Valiunas, 2002). Since I_j of Cx26–Cx32 channels exhibit a residual state at positive voltage only, it follows that Cx26 and Cx32 hemichannels are gating with opposite polarity. This prediction concurs with the conclusions derived from a study on pairs of injected *Xenopus* oocytes, i.e. Cx26 and Cx32 hemichannels are gating with positive and negative polarity, respectively (Verselis et al., 1994).

2.3. Channel concept

These observations have led to a generalised picture for the operation of gap junction channels. Each channel exhibits a voltage-sensitive gating mechanism consisting of two gates in series responsive to transjunctional voltages. Each hemichannel contributes six subgates attributable to the six connexin subunits. The gap junction channel undergoes fast transitions (<2 ms) between the main state, the substates, and the residual state. The probability of a single channel to be in the open state is controlled by V_j. At small V_j, P_o is close to one, at large V_j, it approaches zero. The decline of I_j with time at large V_j is determined primarily by P_o and, to a lesser degree, by the substates. The residual state may be regarded as the ground state of electrical gating. The conductances of both the main state and the residual state are V_j-sensitive. The voltage sensitivity of the hemichannel conductance explains the rectification seen in homomeric-heterotypic gap junctions.

3. Mathematical model

3.1. Motivation

Why should one establish mathematical models in biosciences? For the modellist, the answer is simple and clear: it is his or her demonstration that he or she has understood the observed phenomena. The experimentalist, particularly in bioscience, owns a more conflicting relationship to the impact of mathematical models. In this context, it is important to point out the difference between fitting and modelling. Fitting characterises the process of adjusting a 'reasonable' mathematical function to data which should be followed by an interpretation of this function and the fitting parameters in the context of the observed phenomena. In contrast to this, modelling comprises the process of finding a mathematical description for the object examined starting from its structural and physico-chemical properties. Of course, modelling is often followed by the fitting of the mathematical description to the experimental data.

The modelling and the experimental work must not be seen as detached processes. On the contrary, the dialogue between model and experiment is very fruitful for both of them. This is our own experience and has been demonstrated previously in bioscience and elsewhere. For example, Beeler and Reuter (1976) presented in their classical paper a mathematical reconstruction of the action potential of ventricular myocardial cells using a straightforward model consisting of four membrane currents carried by different ion channels. The differences between the simulated and experimentally measured action potential evoked an avalanche of experimental and theoretical work aimed at extending the knowledge of action potential generation and propagation in the heart. Experiments demonstrated new ionic channels in myocytes located in the cell membrane and the sarcoplasmatic reticulum. Their subsequent mathematical description led to more sophisticated and realistic models like the one by Luo and Rudy (1991).

The possibility of investigating single channels of gap junctions provided complex data on their biophysical behaviour. However, due to the lack of valid models, these data were difficult to interpret. Furthermore, experiments are costly and their outcome is difficult to predict. Thus, in order to optimise the impact of experiments and their results, there was a need for a theoretical model and a simulation tool.

The present section deals with the mathematical modelling of biophysical properties of gap junctions and its application to the design of experiments and the interpretation of the resulting data. Electrophysiological measurements of conductances and kinetics of homomeric-homotypic and homomeric-heterotypic channels at the single channel and multichannel levels (see Section 2) provide the experimental basis of the model. Due to the lack of heteromeric channel data, they could not be included in the model. A generalised mathematical model has been deduced which covers the complete spectrum of channels with their distinct biophysical properties. The modelling process facilitated the understanding of channel mechanisms and hence enabled an easier interpretation of complex data as demonstrated in the case of heterotypic channels (Bukauskas et al., 1997) and the ion selectivity of gap junctions (Valiunas et al., 2000). The model was programmed as a software module that supports the design and selection of promising experimental protocols, thus providing a powerful tool to plan future investigations.

3.2. Existing models

There are several models in the literature which describe the morphological structure of connexins, connexons and gap junction channels (Kumar and Gilula, 1996). Other structural models led to ideas about the putative gating mechanism of the channel (Unwin, 1987). In contrast, there are only few reports which attempt to model the biophysical properties of gap junctions. These models focus on the kinetic aspects and neglect the conductive behaviour of the single channel (Harris et al., 1981; Ramanan et al., 1998; Chen-Izu et al., 2001).

Harris et al. (1981) derived their mathematical model based on multichannel measurements. Due to the lack of experimental data on single channels, they adopted a single channel model consisting of a constant resistor with two gates, one at each end of the resistor. The single channel was considered to have two states, an open state with both gates open and a closed state with one of the gates closed. In order to reproduce the experimental data, the state with both gates closed had to be excluded, i.e. the gates were not assumed to work independently. However, as shown above (see Section 2), the data of single channel conductances and kinetics do not confirm these assumptions and thus the Harris–Spray–Bennett model has lost its validity.

Chen-Izu et al. (2001) recently published a model that describes the kinetic properties of gap junctions. They used a four-state model for the single channels identical to our model (Vogel and Weingart, 1998). In contrast to our approach, thermodynamic considerations have been used to describe the kinetic behaviour. These authors also neglected the impact of single channel conductance properties on the evaluation of the kinetic data.

3.3. Assumptions

The first gap junction model proposed by Harris et al. (1981) relied on macroscopic currents measured in pairs of blastomeres isolated from amphibian embryos. To explain their data, the authors postulated that gap junction channels have two voltage-sensitive gates in series, one located in each hemichannel. Owing to the symmetrical arrangement, the gates respond to voltages of opposite polarity. In addition, it was assumed that each hemichannel has two conductance states, an open state and a closed state. At small transjunctional voltages, V_j, both gates were assumed to dwell in the open state while changing to large voltages V_j, one of the gates is being closed. Hence, their model of a gap junction channel showed three conformational states. In the open state, each gate senses half of V_j while in the closed states, the entire voltage V_j develops across the closed gate and none across the open gate. Consequently, the closed gate of a channel must open before the open sister gate can sense a voltage drop and thus may close.

In contrast to this concept, it is now clear that single channels do not close completely in the presence of large transjunctional voltages. Instead, they flicker between two non-zero conductance states, the main state $\gamma_{j,main}$ and the residual state $\gamma_{j,residual}$. To account for this, we assumed that hemichannels cannot close completely (*first assumption*) and parts of V_j are sensed by both gates irrespective of the conformational state of the channel. These voltage drops govern the gating behaviour of each hemichannel. This may be performed by a specialised domain of the proteinous structure that is able to sense the electrical field inside each hemichannel. Consequently, we gave up the prerequisite of

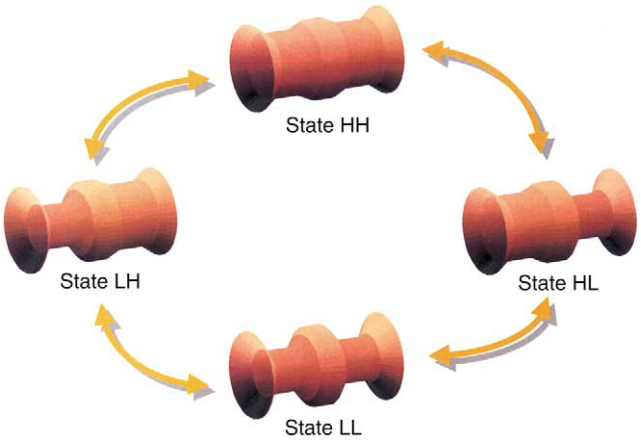

Fig. 3. Three-dimensional model for a single gap junction channel. Relationship between the four conformational states and the three conductive states. State HH corresponds to the main state, states LH and HL correspond to the residual state depending on whether the left or right-hand gate is partially closed. State LL models the functionnal state with both hemichannels partially closed.

dependent gating (*second assumption*) and, in order to propose a general model, a fourth conformational state was tolerated with the gates of both hemichannels partially closed. The second assumption, i.e. independent gating, is supported by the necessity of a functional link between the two gates of the hemichannels to guarantee dependent gating and thus excluding the possibility of the fourth state. Fig. 3 depicts our basic four-state model.

Derived from the molecular structure of the channels, single channel properties are the sum of the properties of their hemichannels (*third assumption*). Hence, the single channel model consists of two submodels linked in series (Fig. 4A). Each submodel represents a hemichannel whose behaviour can be described mathematically (Fig. 4B). For our model, we assumed an exponential relation between the hemichannel conductance and the voltage drop across the hemichannel (*fourth assumption*, Fig. 4B). This assumption was based on the following observations. Experiments on homomeric-heterotypic gap junction channels indicated that $\gamma_{j,main}$ does not obey Ohm's law, i.e. it depends on the amplitude and polarity of V_j. This was discernible in channels consisting of hemichannels with largely different conductances (Cx26–Cx32: Bukauskas et al., 1995b; Cx30–Cx50: Valiunas and Weingart, unpublished; Cx46–Cx50: Hopperstad et al., 2000). Recently, this prediction was verified by direct examination of single hemichannels. The resulting currents revealed a non-linear relationship between the hemichannel conductance and the membrane potential (Trexler et al., 1996; Valiunas and Weingart, 2000), which was best approximated by a single exponential function.

Owing to their absence or rare occurrence, it is impossible or difficult to determine $\gamma_{j,residual}$ at small values of V_j. Hence, there is some uncertainty about the course of the conductance of a partially closed hemichannel. To overcome this deficiency, we assumed that the hemichannel conductance of the

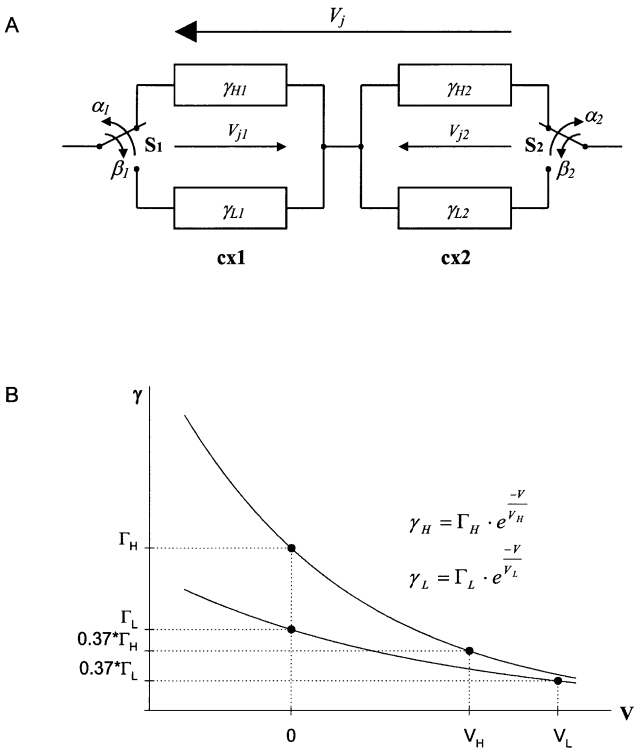

Fig. 4. Single channel model and hemichannel conductances. (A) generalised electrical scheme of a gap junction channel consisting of two hemichannel submodels linked in series. (B) equations and curves representing the conductance–voltage relationship of the high (γ_H, upper trace) and low (γ_L, lower trace) states of a hemichannel. Γ_H, Γ_L: constant multipliers of exponential functions; V: voltage across a hemichannel; V_H, V_L: decay constants at which γ_H and γ_L decline to e^{-1} (from Vogel and Weingart, 1998).

partially closed state follows an exponential course as well (*fifth assumption*, Γ_L in Fig. 4B). The rationale was that the switching of a hemichannel from the open state to a partially closed state merely alters the multiplier and the decay constant of the exponential function without affecting the principle form of the conductance-voltage relationship of the hemichannel. In other words, our concept of channel gating envisions a change in the electrical and/or geometrical properties of the aqueous pore.

Homomeric hemichannels consist of six identical connexins and thus are considered to contain six identical V_j-sensitive subgates. Provided the subgates operate independently, one may expect to see appropriate conductances. Indeed, studies on gap junction channels of vertebrates revealed several interposed states between the main open state and residual state (Valiunas et al., 1996). However, due to the scarcity of quantitative data, these events were not included in the model (*sixth assumption*). Substates are rather rare, i.e. they are preferentially seen early during V_j pulses and at intermediate voltages. Hence, their omission may not seriously impair the validity of the model. It is to mention here that the proposed model is ready to incorporate substates and is able to model their behaviour by the same approach as detailed below.

The membrane potentials of the cells are ignored in this model because the conductive and kinetic properties of vertebrate gap junctions are assumed to be insensitive to the membrane potential (*seventh assumption*) (Waltzman and Spray, 1995; Bruzzone et al., 1996) and we consider the transjunctional voltage V_j to be the sole independent variable of the system. Finally, morphological observations showed that gap junctions are assemblies of single channels. Thus, we assumed that their properties can be calculated by adding up single channels (*eighth assumption*).

3.4. Basic model

The above assumptions are incorporated into the following model (Vogel and Weingart, 1998). A single channel consists of two hemichannels in series (Fig. 4A) and each hemichannel exhibits two conformational states, a high state (H) and a low state (L) of conductance. States H and L correspond to a fully open and a partially closed hemichannel with the assigned conductances γ_H and γ_L, respectively (Fig. 4). The main state of a single channel corresponds to two fully open hemichannels, i.e. both hemichannels in state H which accords with state HH in Fig. 3. The single channel operates in the residual state when either hemichannel 1 (cx1) or hemichannel 2 (cx2) dwells in state L (Fig. 4A). This is very crucial and implies that the single channel residual state has to be represented by two different conformational states. Depending on the polarity of the transjunctional voltage, V_j, the conformational state of the single channel corresponds to state LH or HL (Fig. 3). So far, these states have not been distinguished, i.e. they were treated as one case. This turned out to be a drawback, especially in the case of homomeric-heterotypic channels consisting of hemichannels with different electrical properties when $\gamma_{j,residual}$ becomes asymmetrical (see Fig. 5D in Bukauskas et al., 1997).

For the purpose of modelling, a more detailed nomenclature was introduced. It uses pairs of letters for the states of a single channel. The first and second letters indicate the states of cx1 and cx2, respectively. Therefore, the main state of a single channel corresponds to state HH and the residual state to states LH and HL (Figs. 3 and 4). Since the gates are assumed to work independently, state LL with both hemichannels partially closed is included. Channel conductances related to this state are not yet described in the literature, presumably because of their rare occurrence, their short duration and the fact that their values are close to conductance measured in the residual state (Fig. 5C, see also below).

The voltage-dependent gating of each hemichannel, i.e. the transition between its high and low states, is modelled by the switches S_1 and S_2 (Fig. 4A). The behaviour of each switch is described by the parameters α and β which are interpreted as lifetimes of states L and H, respectively. We proposed that the switches work independently (see the second assumption above) and considered the gating as an intrinsic property of the hemichannels, i.e. each hemichannel has a 'sensor' which detects the local electrical field. This field depends on the voltage drop across the hemichannel. Thus, α_1 and β_1 are functions of V_{j1} and α_2 and β_2 are functions of V_{j2}. The independence of the switches is restricted by the fact that V_{j1} and V_{j2} depend on V_j and the hemichannel conductances (Fig. 4A).

To further discuss conductive and kinetic characteristics of gap junctions, it is important to illustrate the relation between structure and function of a channel. Structurally, there are two classes of channels to consider, homomeric-homotypic and homomeric-heterotypic channels. Each hemichannel exhibits two conductive states thus leading to four channel states (Fig. 3). Overall, this results in eight different cases to deal with. However, for the purpose of the mathematical modelling, these eight cases can be reduced to only two different functional states, called the homotypic and heterotypic function.

The homotypic function is appropriate when both hemichannels possess equal conductive properties which holds true for states HH and LL of a homotypic single channel. This is depicted in Fig. 5A where the dotted exponential curves represent symmetric hemichannels with identical conductive properties, i.e. identical multiplier ($\Gamma_0 = \Gamma_{H1} = \Gamma_{H2}$ or $\Gamma_0 = \Gamma_{L1} = \Gamma_{L2}$) and decay constant ($V_0 = V_{H1} = V_{H2}$ or $V_0 = V_{L1} = V_{L2}$). The total conductance (Fig. 5A, solid line) of such an arrangement is calculated using the formula below (Vogel and Weingart, 1998):

$$\gamma_{tot} = \frac{\Gamma_0}{\exp\left(\frac{-V_j}{V_0\left(1+\exp\left(\frac{V_j}{V_0}\right)\right)}\right) + \exp\left(\frac{V_j}{V_0\left(1+\exp\left(\frac{-V_j}{V_0}\right)\right)}\right)} \quad (1)$$

This function represents a bell-shaped curve symmetrical with respect to the ordinate. The fitting of Equation (1) to experimental data yields the parameters Γ_0 and V_0. They are interpreted as Γ_H and V_H or as Γ_L and V_L when data of main state or state LL are fitted, respectively.

The heterotypic function corresponds to the total conductance of two hemichannels with different conductive functions, i.e. Γ_{01}, V_{01} and Γ_{02}, V_{02} (Fig. 5B, dotted lines). The heterotypic function describes states LH and HL of a homotypic channel and in general, all the four states of a heterotypic channel. Since there is no analytical solution to calculate the total conductance (Fig. 5B, solid line), this case has to be solved numerically (Vogel and Weingart, 1998). In contrast to the homotypic function, the heterotypic function is asymmetric.

In summary, a homotypic channel owns for functions, two homotypic (Fig. 5C, topmost and lowest line) and two heterotypic ones (Fig. 5C, middle two lines) while a heterotypic channel consists of four heterotypic functions (Fig. 5D). The conductances involved are named γ_{HH}, γ_{LH}, γ_{HL} and γ_{LL} in accordance with the channel states HH, LH, HL and LL, respectively.

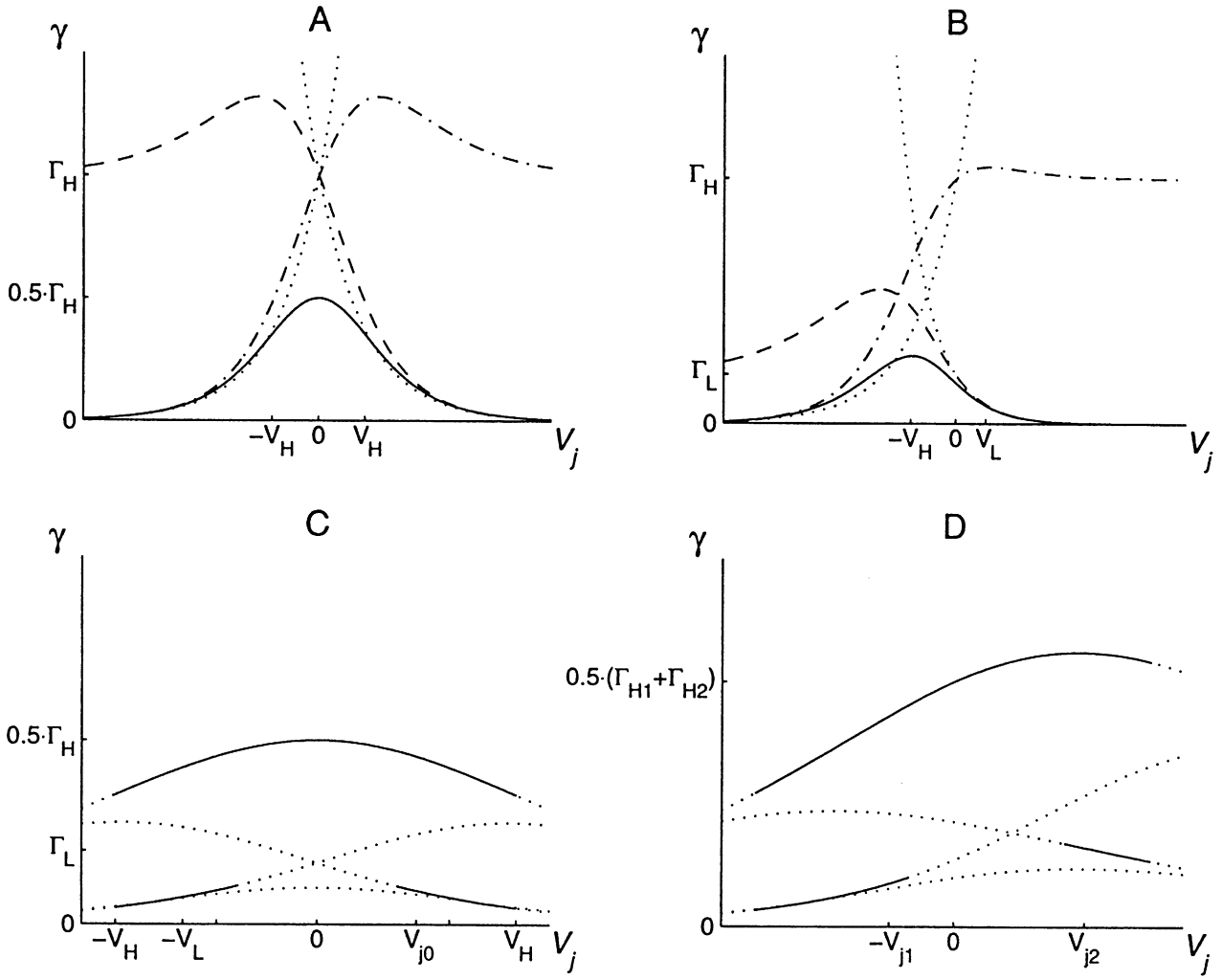

Fig. 5. From homotypic and heterotypic functions to channel conductance. Parameters are in relative units to emphasise the genuine behaviour of the model. (A) a channel consisting of two hemichannels with identical properties generates homotypic conductance functions (dotted lines: hemichannel conductances vs. hemichannel voltage drop; dash–dotted line, dashed line: conductance of hemichannels cx1 and cx2, respectively, vs. transjunctional voltage, V_j ; solid line: total conductance). (B) a channel consisting of two hemichannels with different properties produces heterotypic conductance functions (dotted lines: hemichannel conductances vs. hemichannel voltage drop; dash–dotted line, dashed line: conductance of cx1 and cx2, respectively, vs. V_j; solid line: total conductance). (C) superposition of kinetic and conductance calculations covering the physiological range of V_j for a homotypic single channel. Conductance description involves two heterotypic and two homotypic functions. (D) superposition of kinetic and conductance calculations covering the physiological range of V_j for a heterotypic channel. Conductance description involves four heterotypic functions (adapted from Vogel and Weingart, 1998).

Regarding substates, it is now obvious that substates are to be described with homotypic functions (identical connexins and equal distribution of functional states on each side) or heterotypic functions (different connexins or different distributions of functional states on each side). Thus, experimental data of substates are easily integrated into the model by adding further homotypic and heterotypic functions. This further indicates that the distribution of substates between main and residual state depends on the transjunctional voltage and is not regularly spaced as previously expected (Valiunas et al., 1996).

The plots in Fig. 5 are the result of simulations with chosen parameters to illustrate the general behaviour of gap junctions. They cannot be gained in this way from single channel measurements and hence do not show all features of the model for two reasons:

(i) Cell membranes tolerate voltages up to about ±150 mV. Yet, fitting of the model to experimental data can lead to decay constants above the physiological limit. In the case of a homotypic Cx40 channel, V_H found to be 240 mV. Thus, by increasing V_j from 0 to 150 mV, the single channel main state conductance only decreases by 13% of its maximum value. Hence, the slight bending of γ_{HH} is easily missed in an experiment which can lead to the impression of a constant $\gamma_{j,main}$. For the calculations of Fig. 5C,D, V_H has been set to the physiological limit. The four conductance curves in each plot represent the limited cut-outs of the respective

homotypic and heterotypic function as delineated in Fig. 5A,B.

(ii) For kinetic reasons, the probability to encounter a certain channel state during an experiment varies over the physiological range of V_j. Since little information is currently available on single channel kinetics, we relied on multichannel data to introduce dynamic aspects in to the model. The mathematical description of gap junction kinetics, i.e. the kinetics of multiple channels, is achieved by interpretation of the parameters α and β as rate constants and the use of classical reaction kinetics to calculate the cycling between states (Vogel and Weingart, 1998). The channels preferentially dwell in state HH for small values of V_j and change to state LH or HL for large negative or positive values of V_j. Thus, the residual state, respectively, the 'sum' of states LH and HL, is seen in the vicinity of the physiological limits of V_j. In contrast, γ_{HH} covers the entire physiological range because a channel always starts flickering from state HH (Fig. 5C,D, solid segments of dotted lines). Furthermore, there are transition zones around the equilibrium voltage, $V_{j,0}$, where the states occur at intermediate probabilities. $V_{j,0}$ is defined as the voltage at which α equals β. They are symmetrical with respect to the ordinate for a homotypic channel and asymmetrical for a heterotypic channel (see Fig. 1C,D; see also Vogel and Weingart, 1998).

The state LL is associated with a fourth channel conductance, γ_{LL}, smaller than the conductance of states LH and HL (bottom line of Fig. 5C,D). The experimental documentation of state LL is difficult because its conductance is very close to the conductance of states LH and HL as shown inFig. 5A,B. Furthermore, simulation studies suggest that the probability of encountering a single channel dwelling in state LL is extremely low and its lifetime short at each V_j. Careful inspection of our data has revealed a state with a conductance smaller than $\gamma_{j,residual}$ but distinctly different from zero. These events were very rare and short. Further investigations are needed to elucidate this issue. Conceivably, the gap junction model presented may help to design a pulse protocol which optimises the probability to detect state LL.

In conclusion, the gap junction model described is versatile. It allows to simulate all types of vertebrate gap junctions currently known. Two hemichannels with exponential conductance–voltage functions, when connected in series, reproduce the *quasi* constant conductance of a homotypic channel as well as the rectifying behaviour of a heterotypic channel. The kinetics are described by two switches governed by the voltage drop across each hemichannel. Single channel and multichannel data can be described with the same formalism. In the single channel situation, the parameters α and β are interpreted as lifetimes of single channel states, in the multichannel situation, as rate constants of I_j inactivation. The model is flexible and can easily be adapted to accommodate results of further investigations. For example, substates could be introduced by adding new conductances or a fully closed state by introducing a zero conductance in parallel. The model can be integrated in systems of higher order, e.g. models of heart cells could be linked with the gap junction model to explore the role of gap junctions during normal and impaired impulse propagation causing cardiac arrhythmias (Henriquez et al., 2001). The gap junction model will help to plan experiments aimed at further elucidating the electrical properties of the channels.

3.5. Implications

Gap junctions may be regarded as filters for the exchange of intercellular signals in multicellular tissues. In view of the types of connexins currently identified, the possibility of the formation of structurally different channels (homomeric-homotypic, homomeric-heterotypic, possibly heteromeric-homotypic and heteromeric-heterotypic) and the dynamic properties inherent to each channel, the number of channels with different functional properties is enormous. Conceivably, nature may make use of many of these possibilities. While the presence of homomeric-homotypic and homomeric-heterotypic gap junctions is well established, the existence of heteromeric-homotypic and heteromeric-heterotypic channels is controversial and awaits unambiguous functional demonstrations (see e.g. Valiunas et al., 1999b; Hopperstad et al., 2000; Cottrell and Burt, 2001; Valiunas et al., 2001; Polontchouk et al., 2002). Conductance data of potential heteromeric channels would further elucidate the role of connexin assemblage on hemichannels function.

Acknowledgements

We thank Dr. W. Cascio, Division of Cardiology, University of North Carolina at Chapel Hill, USA, for critical comments and hospitality. Part of the writing was done in his laboratory. This study was supported by the Swiss National Science Foundation (31-55297.98 and 31-67230.01).

References

Beeler, W., Reuter, H., 1976. Reconstruction of the action potential of ventricular myocardial fibres. J. Physiol. 268, 177–210.

Bruzzone, R., White, T.W., Paul, D.L., 1996. Connections with connexins; the molecular basis of direct intercellular signalling. Eur. J. Biochem. 238, 1–27.

Bukauskas, F.F., Elfgang, C., Willecke, K., Weingart, R., 1995a. Biophysical properties of gap junction channels formed by mouse connexin40 in induced pairs of transfected human HeLa cells. Biophys. J. 68, 2289–2298.

Bukauskas, F.F., Elfgang, C., Willecke, K., Weingart, R., 1995b. Heterotypic gap junction channels (connexin26–connexin32) violate the paradigm of unitary conductance. Pflügers Arch. 429, 870–872.

Bukauskas, F.F., Vogel, R., Weingart, R., 1997. Biophysical properties of heterotypic gap junctions newly formed between two types of insect cells. J. Physiol. 499, 701–713.

Bukauskas, F.F., Weingart, R., 1994. Voltage-dependent gating of single gap junction channels in an insect cell line. Biophys. J. 67, 613–625.

Chen-Izu, Y., Moreno, A.P., Spangler, R.A., 2001. Opposing gates model for voltage gating of gap junction channels. Am. J. Physiol. 281, C1604–C1613.

Condorelli, D.F., Parenti, R., Spinella, F., Trovato Salinaro, A., Belluardo, N., Cardile, V., Cicirata, F., 1998. Cloning of a new gap junction gene (Cx36) highly expressed in mammalian brain neurons. Eur. J. Neurosci. 10, 1202–1208.

Cottrell, G.T., Burt, J.M., 2001. Heterotypic gap junction channel formation between heteromeric and homomeric Cx40 and Cx43 connexons. Am. J. Physiol. 281, C1559–C1567.

Ek-Vitorin, J.F., Calero, G., Morley, G.E., Coombs, W., Taffet, S.M., Delmar, M., 1996. PH regulation of connexin43: molecular analysis of the gating particle. Biophys. J. 71, 1273–1284.

Harris, A.L., 2001. Emerging issues of connexin channels: biophysics fills the gap. Quart. Rev. Biophys. 34, 325–472.

Harris, A.L., Spray, D.C., Bennett, M.V.L., 1981. Kinetic properties of a voltage dependent junctional conductance. J. Gen. Physiol. 77, 95–117.

Henriquez, A.P., Vogel, R., Muller-Borer, B.J., Henriquez, C.S., Weingart, R., Cascio, W.E., 2001. Influence of dynamic gap junction resistance on impulse propagation in ventricular myocardium: a computer simulation study. Biophys. J. 81, 2112–2121.

Hopperstad, M.G., Srinivas, M., Spray, D.C., 2000. Properties of gap junction channels formed by Cx46 alone and in combination with Cx50. Biophys. J. 79, 1954–1966.

Kumar, N.M., 1999. Molecular biology of the interactions between connexins. Gap Junction-Mediated Intercellular Signalling in Health and Disease, Novartis Foundation Symposium 219. Wiley, New York, pp. 6–16.

Kumar, N.M., Gilula, N.B., 1996. The gap junction communication channel. Cell 84, 381–388.

Luo, C., Rudy, Y., 1991. A model of the ventricular cardiac action potential. Circ. Res. 68, 1501–1525.

Polontchouk, L.O., Valiunas, V., Haefliger, J.A., Eppenberger, H.M., Weingart, R., 2002. Expression and regulation of connexins in cultured ventricular myocytes isolated from adult rat hearts. Pflügers Arch. 443, 676–689.

Purnick, E.M., Oh, S., Abrams, C.K., Verselis, V.K., Bargiello, T.A., 2000. Reversal of the gating polarity of gap junctions by negative charge substitutions in the N-terminus of connexin 32. Biophys. J. 79, 2403–2415.

Ramanan, S.V., Brink, P.R., Varadaraj, K., Peterson, E., Schirrmacher, K., Banach, K., 1998. A three-state model for connexin37 gating kinetics. Biophys. J. 76, 2520–2529.

Rüdisüli, A., Weingart, R., 1989. Electrical properties of gap junction channels in guinea-pig ventricular cell pairs revealed by exposure to heptanol. Pflügers Arch. 415, 12–21.

Sohl, G., Degen, J., Teubner, B., Willecke, K., 1998. The murine gap junction gene connexin36 is highly expressed in mouse retina and regulated during brain development. FEBS Lett. 428, 27–31.

Trexler, E.B., Bennett, M.V.L., Bargiello, T.A., Verselis, V.K., 1996. Voltage gating and permeation in a gap junction hemichannel. Proc. Natl. Acad. Sci. USA 93, 5836–5841.

Trexler, E.B., Bukauskas, F.F., Kronengold, J., Bargiello, T.A., Verselis, V.K., 2000. The first extracellular loop is a major determinant of charge selectivity in connexin46 channels. Biophys. J. 79, 3036–3051.

Unger, V.M., Kumar, N.M., Gilula, N.B., Yaeger, M., 1999. Electron cryocrystallography of a recombinant cardiac gap junction channel. Gap Junction-Mediated Intercellular Signalling in Health and Disease, Novartis Foundation Symposium 219. Wiley, New York, pp. 6–16.

Unwin, P.N., 1987. Gap junction structure and the control of cell-to-cell communication. Junctional Complexes of Epithelial Cells, Ciba Foundation Symposium. Wiley, New York, pp. 78–91.

Valiunas, V., 2002. Biophysical properties of connexin-45 gap junction hemichannels studied in vertebrate cells. Biophys. J. 119, 147–164.

Valiunas, V., Bukauskas, F.F., Weingart, R., 1997. Conductances and selective permeability of connexin43 gap junction channels examined in neonatal rat heart cells. Circ. Res. 80, 708–719.

Valiunas, V., Gemel, J., Brink, P.R., Beyer, E.C., 2001. Gap junction channels formed by coexpressed connexin40 and connexin43. Am. J. Physiol. 281, H1675–H1689.

Valiunas, V., Manthey, D., Willecke, K., Weingart, R., 1996. Electrical properties of connexin30 gap junction channels studied in transfected HeLa cells. Pflügers Archiv 431, R93.

Valiunas, V., Manthey, D., Vogel, R., Willecke, K., Weingart, R., 1999a. Biophysical properties of mouse connexin30 gap junction channels studied in transfected human HeLa cells. J. Physiol. 519, 631–644.

Valiunas, V., Niessen, H., Willecke, K., Weingart, R., 1999b. Electrophysiological properties of gap junction channels in hepatocytes isolated from connexin32-deficient and wild-type mice. Pflügers Arch. 437, 846–856.

Valiunas, V., Vogel, R., Weingart, R., 2000. The kinetics of gap junction currents are sensitive to the ionic composition of the pipette solution. Pflügers Arch. 440, 835–842.

Valiunas, V., Weingart, R., 2000. Electrical properties of gap junction hemichannels identified in transfected HeLa cells. Pflügers Arch. 440, 366–379.

Verselis, V.K., Ginter, C.S., Bargiello, T.A., 1994. Opposite voltage gating polarities of two closely related connexins. Nature 368, 348–351.

Vogel, R., Weingart, R., 1998. Mathematical model of vertebrate gap junctions derived from electrical measurements on homotypic and heterotypic channels. J. Physiol. 510, 177–189.

Waltzman, M.N., Spray, D.C., 1995. Exogenous expression of connexins for physiological characterisation of channel properties: comparison of methods and results. In: Kanno, Y., Kataoka, K., Shiba, Y., Shibata, Y., Shimazu, T. (Eds.), International Communication Through Gap Junctions. Progress in Cell Research, vol. 4. Elsevier, Amsterdam, pp. 9–17.